Title: Novel coumarin-pyridazine hybrids as selective MAO-B inhibitors for the Parkinson's disease therapy

Fernanda Rodríguez-Enríquez [a,b], María Carmen Costas-Lago [c], Pedro Besada [c], Miguel Alonso-Pena [c], Iria Torres-Terán [a,b], Dolores Viña [a,b], José Angel Fontenla[b], Mattia Sturlese [d], Stefano Moro [d], Elias Quezada[e], Carmen Terán [c *]

[a] Centro de Investigación en Medicina Molecular y Enfermedades Crónicas (CIMUS) Universidade de Santiago de Compostela,15706 Santiago de Compostela, Spain
[b] Departamento de Farmacología, Farmacia y Tecnología Farmacéutica, Facultad de Farmacia, Universidade de Santiago de Compostela, 15782 Santiago de Compostela, Spain
[c] Departamento de Química Orgánica e Instituto de Investigación Sanitaria Galicia Sur (IISGS), Universidade de Vigo, 36310 Vigo, Spain
[d] Molecular Modeling Section (MMS), Dipartimento di Scienze del Farmaco, Università degli Studi di Padova, 35131, Padova, Italy.
[e] Departamento de Química Orgánica, Facultad de Farmacia, Universidade de Santiago de Compostela, 15782 Santiago de Compostela, Spain.

* Corresponding author.

Phone: 34 986 812276
E.mail: mcteran@uvigo.es

ABSTRACT

The 3-pyridazinylcoumarin scaffold was previously reported as an efficient core for the discovery of reversible and selective inhibitors of MAO-B, a validated drug target for PD therapy which also plays an important role in the AD progress. Looking for its structural optimization, novel compounds of hybrid structure coumarin-pyridazine, differing in polarizability and lipophilicity properties, were synthesized and tested against the two MAO isoforms, MAO-A and MAO-B (compounds **17a-f** and **18a-f**).

All the designed compounds selectively inhibited the MAO-B isoenzyme, exhibiting many of them IC_{50} values ranging from sub-micromolar to nanomolar grade and lacking neuronal toxicity. The 7-bromo-3-(6-bromopyridazin-3-yl)coumarin (**18c**), the most potent compound of these series (IC_{50} = 60 nM), was subjected to further *in vivo* studies in a reserpine-induced mouse PD model. The obtained results suggest a promising potential for **18c** as antiparkinsonian agent.

Molecular modeling studies also provided valuable information about the enzyme-drug interactions and the potential pharmacokinetic profile of the novel compounds.

Keywords: coumarin-pyridazine hybrids, MAO-B, Parkinson's disease, *in vivo* study, SAR study.

1. Introduction

The term neurodegenerative diseases (ND) refers to a heterogeneous group of pathologies affecting the nervous system which occur with a selective and gradual loss of neurons, damaging the mental and physical skills of people suffering them. The ND as an important part of age-related disorders, are becoming a major public health issue.

Alzheimer's (AD) and Parkinson's disease (PD) are the most usual types of ND, since it is estimated that millions of people over 65 years worldwide currently suffer from one of these disorders, and their prevalence is even growing mainly with the improvement in life expectancy [1]. In AD the affected brain regions are hippocampus, cortex and neocortex, leading to dementia, while in PD the dopaminergic neurons of the substantia nigra are destroyed resulting in a significant dopamine deficiency in striatum giving rise to a movement disorder which affects both motor and non-motor functions [2]. Although ageing is the main risk factor for suffering from AD or PD, the aetiology of both disorders is also linked to environmental, genetic, epigenetic factors and even to unknown ones. Among the different and complex pathogenic mechanisms involved in neurodegeneration, such as oxidative stress, disturbance in neurotransmitter levels, neuro-inflammation, mitochondrial dysfunction, excitotoxicity, the proteolytic stress, related to misfolded protein oligomers and their deposition in brain causing neuronal death, seems to play a key role on pathology and progression of AD and PD [2,3]. These types of protein aggregates can be considered the hallmarks for the diagnosis of AD and PD in post-mortem brains [4].

The complex physiopathology of these disorders makes difficult the discovery of new therapies contributing to prevent or completely reverse their progression, and at the same time promotes the research on new drugs with the ability to block or reduce some important events involved in neurodegeneration [1,5].

The current therapy for PD is mainly focused on treating the motor impairments enhancing the striatal dopaminergic activity by increasing dopamine levels or stimulating dopamine receptors. In this regard, the approved drugs comprise dopamine precursors as levodopa (L-dopa, **1**), which is often prescribed in combination with carbidopa (**2**) or benserazide (**3**) in order to reduce its metabolism at peripheral tissues, dopamine receptors agonists, such as apomorphine (**4**) and pramipexole (**5**) (Figure 1) and inhibitors of enzymes involved in dopamine catabolism, in particular selective monoamine oxidase B (MAO-B) inhibitors, such as selegiline (**6**), rasagiline (**7**) or

safinamide (**8**), and catechol-*o*-methyl transferase (COMT) inhibitors as entacapone (**9**), tolcapone (**10**) and opicapone (**11**) (Figure 2) [4,6]. Selegiline and rasagiline are two irreversible MAO-B inhibitors, while safinamide, recently approved by Food and Drug Administration (FDA) as antiparkinsonian drug, is a reversible MAO-B inhibitor [7]. The reversible MAO-B inhibition avoids the possible immunogenic side effects derived from the covalent binding of the drug to the flavin cofactor of the enzyme [8].

Figures 1 and 2 come about here

There are several reasons that justify the therapeutic potential of MAO-B inhibitors against PD or even against AD, as for instance the increase of MAO-B activity in the human brain with ageing, and specifically in people suffering from PD or AD [7], giving rise to a disturbance in neurotransmitter levels together with an excess of toxic free radicals, causing mitochondrial damage that results in neuronal death. In addition, a number of experimental parkinsonian models have shown the neuroprotective effects of MAO-B inhibition [9]. Taking into account that MAO-B inhibitors require a certain amount of dopamine to perform their function, these drugs will be effective as monotherapy in the first steps of PD and as L-dopa adjuvants in advanced stages of the disease, allowing the reduction of L-dopa dose or even delaying the use of high doses. Clinical trials have evidenced a possible relationship between the L-dopa sparing properties of MAO-B inhibitors and their neuroprotective effects [10]. However, there is a general opinion that cellular mechanisms not related to neurotransmitters degradation would be involved in the neuroprotective properties of these compounds [8]. Likewise, recent clinical trials performed with AD patients point out a beneficial effect of MAO-B inhibition on the behavioural and neuropsychiatric symptoms, which are associated with the fast progression of the illness to severe dementia [11].

The coumarin is a heterocyclic core present in both natural and synthetic compounds, which displays a very attractive profile for drug discovery due to the variety of biological properties of its derivatives [12]. Recent research works demonstrated the potential of the coumarin nucleus for the development of compounds with MAO-B selectivity [13]. Among its different substitution patterns, the 3-arylcoumarin scaffold has a special relevance, because it has provided some of the most potent and selective *in vitro* human MAO-B (hMAO-B) inhibitors described so far, such as the 6-methyl-3-(4-methylphenyl)coumarin (**12**), the 3-(3-bromophenyl)-6-methylcoumarin (**13**) and the 3-

(4-bromophenyl)-6-methoxycoumarin (**14**), all them with IC_{50} values of sub-nanomolar grade (Figure 3) [14]. In addition, the substitution of the phenyl group at C3 by several heterocyclic rings provided also selective hMAO-B inhibitors [15]. Some of the 3-heteroarylcoumarins containing the pyridazine core at C3 were active at sub-micromolar concentration when a bromine atom was placed at the pyridazine ring and a methoxy or a methyl group was located at C6 or C7 (compounds **15** and **16**) of the coumarin nucleus [15b]. In addition, these coumarin-pyridazine hybrid compounds were devoid of neurotoxic effects at active concentration and behaved as reversible MAO-B inhibitors with good theoretical pharmacokinetic properties.

Figure 3 comes about here

The results obtained with the 3-pyridazinylcoumarins encourage us to further study this scaffold trying to optimize the structure by removing the methyl or methoxy group at the benzene ring of the coumarin nucleus or replacing them by a halogen atom (Cl or Br), in order to modify the polarizability and lipophilicity properties of the coumarin fragment and with it the possible interactions with the enzyme. The structure of the new designed and synthesized 3-pyridazinylcoumarins was detailed in Figure 3 (compounds **17**-**18**). The MAO inhibitory activity of target compounds was studied *in vitro* using recombinant human MAO-A and MAO-B in order to determine their potency and selectivity profile. In addition, computational and *in vivo* studies were also performed to achieve a better comprehension of their binding modes, estimate their druggability and get more reliable information about their potential for PD therapy.

2. Results and discussion

2.1. *Chemistry*

The coumarin-pyridazine hybrids **17a-f** and **18a-f** were efficiently synthesized applying a versatile methodology in which the Knoevenagel condensation of pyridazinone ester **19** [15b] with the corresponding *o*-hydroxybenzaldehyde was the key step (Scheme 1).

Scheme 1 comes about here

The Knoevenagel reaction of **19** with *o*-hydroxybenzaldehyde (**20a**) or several *o*-hydroxybenzaldehydes displaying a chlorine or bromine atom at different positions of

the benzene ring (**20b-f**), all of them available in the market, was conducted with piperidine in 2-propanol at reflux and provided in good yields (73-87%) a set of coumarin cores containing the pyridazinone fragment at C3 (compounds **21a-f**) [16].

Finally, in order to obtain the novel coumarin-pyridazine hybrids **17** and **18**, compounds **21** were subjected to a chemoselective chlorination or bromination applying two previously established methods [15b]. Thus, the 3-(6-chloropyridazin-3-yl)coumarins **17a-f** were achieved in moderate yield (51-64%) by refluxing the pyridazinone-coumarins **21a-f** with $POCl_3$. In the same way, the treatment of **21a-f** with $POBr_3$ in toluene at reflux provided the 3-(6-bromopyridazin-3-yl)coumarins **18a-f** in moderate to good yield (48-95%).

2.2. *MAO inhibition in vitro studies*

All the target compounds of hybrid structure coumarin-pyridazine were studied *in vitro* to know their effect on the two MAO isoforms activity using recombinant human MAO-A and MAO-B isoenzymes expressed in insect cells infected by baculovirus. This screening was performed through the Amplex® red MAO assay and following a previously instituted protocol [14-15]. The data of the inhibitory effects (IC_{50} values) and selectivity MAO-B of these new series of coumarin-pyridazine hybrids and reference drugs, selegiline and iproniazide, are detailed in Table 1. In order to better analyze the structure-activity relationships of these new series of coumarin-pyridazine hybrids, Table 1 also includes the IC_{50} values of 3-(6-bromopyridazin-3-yl)coumarins **15** and **16** previously mentioned as starting point of this work.

All the compounds designed in this study selectively inhibited the MAO-B isoenzyme without affecting the MAO-A isoform activity at the highest evaluated concentration (100 μM). In addition, many of the synthesized halopyridazinylcoumarins exhibited IC_{50} values ranging from sub-micromolar to nanomolar grade.

In general terms and with exception of compound **17d**, it has been observed that a bromine atom linked to the pyridazine ring led to MAO-B inhibitors more potent and selective than a chlorine atom located in the same position. This assessment is consistent with the results previously obtained for the series of pyridazinylcoumarins displaying a methoxy or methyl group at the coumarin core [15b].

As it was depicted in Table 1, the 3-(6-chloropyridazin-3-yl)coumarin **17a** is the least active compound of these series. The introduction of a halogen atom (Cl or Br) in the coumarin nucleus of compound **17a** improved the MAO-B inhibitory activity over 2.3

to 249 times depending on the type of halogen and its position in the coumarin fragment (compounds **17b-f**). The best results of potency and selectivity were obtained with the 7-bromo (**17c**) and 8-bromo (**17d**) coumarin isomers, with IC_{50} values of 0.17 and 0.97 μM, respectively.

The 3-(6-bromopyridazin-3-yl)coumarin **18a**, without any additional substituent at the coumarin framework, exhibited a MAO-B inhibitory potency (IC_{50} = 0.99 μM) almost comparable to that of its 6-methoxy and 7-methyl coumarin analogues, compounds **15** (IC_{50} = 0.56 μM) and **16** (IC_{50} = 0.75 μM), respectively. However, the introduction of an extra halogen atom at C6, C7 or C8 of the coumarin core, which resulted in compounds **18b-f**, remarkably affected the MAO-B potency and selectivity. Thus, whereas the placement of a chloride group at C6 (**18e**) or C8 (**18f**) or a bromide group at C8 (**18d**) decreased the activity, especially when it is the 6-chloro coumarin isomer **18e** (IC_{50} = 10.22 μM), a slight increase of potency and selectivity was observed when the bromide group was located at C6 (**18b**, IC_{50} = 0.36 μM), which became much more significant for the 7-bromo coumarin isomer **18c** (IC_{50} = 0.06 μM). The results of this study point out that compound **18c** is a hMAO-B inhibitor more active than iproniazide, and with a potency in the range of selegiline (IC_{50} = 0.02 μM), displaying also a high selectivity index versus the hMAO-B isoform.

Table 1 comes about here

The compound **18c** was selected to corroborate the type of inhibitory effect. A reversibility study was performed applying a validated dilution method [15b,17] and using as reference drugs an irreversible and a reversible inhibitor, selegiline and isatin, respectively. The obtained results indicated that compound **18c** behaves like a reversible inhibitor, although to a lesser extent than isatin (Table 2).

Table 2 comes about here

2.3. *Cell toxicity studies*

Taking into account the above mentioned results, and in order to know the possible neuronal toxicity of the novel coumarin-pyridazine hybrids **17-18**, cytotoxicity studies were performed by using the human neuronal cell line SH-SY5Y. The cytotoxic effects

were analysed at a concentration of 10 μM, and the cell viability percentage was evaluated by the MTT assay [15b,18].

As shown on Figure 4, only the 8-bromo-3-(6-chloropyridazin-3-yl)coumarin (**17d**, IC_{50} = 0.97 μM) appreciably reduced the SH-SY5Y cell line viability at 10 μM. Most of the studied coumarin-pyridazine hybrids lack cellular toxicity at the tested concentration, suggesting that can be safe MAO-B agents.

The data collected from the *in vitro* studies promoted the *in vivo* study of compound **18c** as a possible candidate for PD therapy.

Figure 4 comes about here

2.4. *In vivo studies*

Effects of **18c** and selegiline (reference drug) on the motor activity were evaluated using the open field test (OFT) in both unpretreated mice and in mice pretreated with reserpine [19].

Unpretreated mice. Doses of 10 mg/kg or 100 mg/kg of compound **18c** administered to mice did not show significant effects on locomotor activity, velocity or percentage of time in movement respect to the control group. By contrast, selegiline, administered at a dose of 10 mg/kg significantly increased the motor activity (Figure 5). These results can be explained because selegiline is metabolized to amphetamine derivatives, as it has been previously described by Engberg and co-workers [20].

Figure 5 comes about here

Potentiation effect L-dopa/benserazide in mice pretreated with reserpine. Neither the treatment with L-dopa/benserazide nor the treatment with selegiline at the evaluated dosage increased the locomotor activity, velocity or percentage of time in movement for these animals. It was the combination of both that manages to increase these parameters. The difference in the motor effects caused exclusively by selegiline, in unpretreated mice (hypermotility) *vs* reserpinized mice (no effect), can be explained by the possibility of the enzymatic inhibition caused by reserpine [21].

Compound **18c** was initially administered at a dose of 100 mg/kg, a dose that unlike selegiline, had no effect on untreated mice. However, in reserpinized mice this dose in association with L-dopa/benserazide achieved a significant increase in the locomotor

activity, velocity or percentage of time in movement in the OFT. Therefore, **18c** was subsequently administered at a dose of 10 mg/kg causing a similar response (Figure 6). After 24 h of monitoring, once the experiment was completed, no mortality was observed in the animals treated with the compound **18c**. These results attribute interesting properties to this compound as a potential antiparkinsonian agent.

Figure 6 comes about here

2.5. *Molecular modeling studies*

Molecular docking studies were carried out to investigate the possible binding mode of the novel coumarin-pyridazine hybrids. To set up a solid docking protocol we firstly focused our attention on selecting an appropriate protein conformation to be used in the calculation and the most suitable docking protocol. Fortunately, in the protein databank, two crystallographic complexes of hMAO-B hosting a coumarin-based ligand (PDB code: 2V60 and 2V61) [22] are available. We concentrated the calculation on those protein conformations more prone to accommodate a similar scaffold. At this point, we performed a benchmark comparing the ability of 17 different docking protocols in reproducing the two selected experimental structures. The benchmark results indicated that generally the complex 2V60 was more accurately reproduced and that Gold-Chemscore showed the best performance (SI Figure 1). Taking advantage of these findings, we docked the twelve synthesized compounds. The results suggest that all the derivatives could theoretically be accommodated in the binding site maintaining the same orientation of the coumarin scaffold in the experimental complex structure. Nevertheless, the position of the coumarin ring is slightly shifted due to the presence of the halogenated pyridazine group in position 3, such bulky substituent is missing in c17. The introduction of this group leads to modifying the pattern of interaction of the coumarin scaffold. Thus, while in c17 a hydrogen bond between the carbaldehyde in position 4 and Tyr435 is given, in most of the novel derivatives such interaction is mediated by the pyridazine. The shift of the coumarin scaffold is due to the steric effect of halogenated pyridazine that faced the Flavin-adenine dinucleotide. The most potent ligand, compound **18c**, in addition to the hydrogen bond with Tyr 435 establishes strong electrostatic interactions with Gln206, Tyr326, and Tyr188. Several hydrophobic contacts are also found, in particular with Phe168, Leu171, Ile199, Ile316, and Tyr326. The bromine atom of the pyridazine is located in a region rich in ring currents formed

by Tyr60, Tyr398, Tyr435, Phe343, and the FAD. The bromine atom in position 6 of the coumarin ring instead, is placed on a hydrophobic pocket formed by Leu164, Trp119, Ile199, Phe103, Pro104, Phe168, and Ile316 (Figure 7).

Figure 7 comes about here

A direct comparison of **18c** with c17 protein-ligand interaction patterns is reported on Figure SI2 and SI3 by analyzing the electrostatic and hydrophobic contribution (IE_{ele}, and IE_{hyd}) of each residue to the interaction energy, which confirms that both compounds share a common binding mode. This study is particularly suitable to analyze and compare the new synthesized derivatives. All the compounds showed similar heat-maps conforming the same orientation they assumed (Video SI 1). The different combination of halogen substituents to the coumarin-pyridazine scaffold slightly perturbs the electrostatic and hydrophobic pattern of interactions. This comparison could help in highlights the molecular basis that may explain the IC_{50} value differences. In fact, we observe that certain residues can establish strong interaction only with the most potent compounds. In particular, the Tyr60 seems to be crucial to explain the activity in our derivatives. A similar situation can be found in the repulsive effect observed between our ligands with Ile198 and Ile199, this unfavorable interaction is more pronounced for less potent derivatives. This trend is also confirmed by docking scores that rank our derivatives similarly to the rank obtained by the IC_{50} data (SI Video 1).

To evaluate the *in silico* ADME-Tox (absorption, distribution, metabolism, excretion, and toxicity) profile of the synthesized compounds a panel of descriptors were calculated and compared with reference inhibitors, selegiline and iproniazide (Table 3). All the compounds showed an acceptable profile, in particular, all of them were predicted to be able to penetrate the blood-brain barrier (BBB) likely the reference inhibitor. All the compounds showed satisfactory scores in the models for the affinity to Cytochrome P450 2D6 and 2C9. The main difference between our derivatives to the reference inhibitors regards the aqueous solubility (log S) that for our compounds is limited respect to the reference. The model that predicts the binding to plasma protein (PPB90 category) reported a different behavior along the series, with some derivative classified as putative with a high probability. On the contrary, 8 derivatives, included

the most potent compound **18c**, showed a reduced binding propensity like the references.

Table 3 comes about here

3. Conclusions

Twelve novel compounds of hybrid structure coumarin-pyridazine were successfully designed and synthetized as selective MAO-B inhibitors. Many of the target compounds exhibited IC_{50} values ranging from sub-micromolar to nanomolar grade. The structure-activity relationship analysis performed evidenced again that the presence of a bromine atom at C6 of the pyridazine ring is very favorable for the activity. Likewise, an important increase in the MAO-B inhibitory effects, both potency and selectivity, was observed when an additional bromine atom was located at the coumarin fragment, in particular at C7, even if the halogen atom at C6 of the diazine ring is a chlorine atom. These results corroborated the key role of halogens in MAO-B inhibition [23].

The performed *in silico* ADME-Tox prediction suggested that all the designed compounds may exhibit suitable drug-like properties. The molecular docking provided insights about the binding mode of the target compounds and revealed some key residues, such as Tyr60, Ile198 and Ile199, as crucial to explain the activity of the novel coumarin-pyridazine hybrids. The 7-bromo-3-(6-bromopyridazin-3-yl)coumarin (**18c**), the most potent compound of theses series displayed *in vitro* MAO-B inhibitory potency (IC_{50} = 60 nM) which is in the range of the selegiline (IC_{50} = 17 nM). In addition, compound **18c** significantly enhances the L-dopa/benserazide effects on motor activity in reserpinized mice, at both doses of 100 mg/kg and 10 mg/kg. Because of its good pharmacological profile, **18c** can be highlighted as a potential antiparkinsonian agent.

4. Experimental section

4.1. General methods and materials

All reagents and common laboratory chemicals were acquired from commercial sources and directly used. All solvents were dried following standard procedures. Melting points were measured in open capillary tubes by using a Stuart Scientific apparatus. ^{1}H and ^{13}C NMR spectra were determined using a Bruker ARX400 instrument and TMS as internal standard [chemical shifts (δ) in ppm, J in Hz]. The assignment of the signals was performed by COSY, DEPT, HSQC experiments. High resolution mass spectra were

obtained from a Bruker microTOF focus spectrometer. Flash chromatography (FC) was carried out on silica gel (Merck 60, 230–400 mesh). Analytical TLC was performed on pre-coated plates of silica gel (Merck 60 F254, 0.25 mm). Microanalyses were performed using a PerkinElmer 240B elemental analyzer. Intermediate compounds **19** and **21a-f** were synthesized as previously was reported [15b, 16]

*4.2. General methodology to synthesize the 3-(6-chloropyridazin-3-yl)coumarins (**17a-f**).*

An excess of $POCl_3$ (2 mL) was added to the corresponding 3-(6-oxo-1,6-dihydropyridazin-3-yl)coumarin **21** (0.36 mmol). The reaction mixture was stirred at reflux 14 h, carefully poured onto ice (~ 1mL) and rendered alkaline with a 25% wt. aqueous solution of NH_3. The precipitate obtained was filtered, rinsed with H_2O and dried to provide the titled compound.

*4.2.1. 3-(6-chloropyridazin-3-yl)coumarin (**17a**).*

Brown solid; yield 51%; R_f = 0.6 (50% EtOAc/hexane); m.p. = 212 - 213 °C; ^{1}H NMR ($CDCl_3$): δ = 9.00 (s, 1H, H4), 8.58 (d, 1H, *J* = 9.1 Hz, H4'), 7.70 (d, 1H, *J* = 7.7 Hz, H5), 7.67 - 7.61 (m, 1H, H7), 7.60 (d, 1H, *J* = 9.1 Hz, H5'), 7.46 – 7.36 (m 2H, H6, H8); ^{13}C NMR ($CDCl_3$): δ = 160.1 (C2), 156.3 (C6'), 154.5, 154.3, 144.2 (C4), 133.5 (C7), 129.6 (C5), 129.3 (C4'), 128.1 (C5'), 125.2 (C6), 121.7 (C3), 119.2 (C4a), 116.8 (C8); HRMS (ESI): *m/z* $[M+H]^+$ calcd for $C_{13}H_8ClN_2O_2$, 259.0269; found 259.0270.

Anal. Calcld for $C_{13}H_7ClN_2O_2$: C, 60.37; H, 2.73; N, 10.83. Found: C, 60.45; H, 2.65; N, 10.90.

*4.2.2. 6-bromo-3-(6-chloropyridazin-3-yl)coumarin (**17b**).*

Brown solid; yield 61%; R_f = 0.6 (50% EtOAc/hexane); m.p. = 256 - 257 °C; ^{1}H NMR ($CDCl_3$): δ = 8.92 (s, 1H, H4), 8.57 (d, 1H, *J* = 9.1 Hz, H4'), 7.84 (d, 1H, *J* = 2.2 Hz, H5), 7.72 (dd, 1H, *J* = 8.8, 2.2 Hz, H7), 7.61 (d, 1H, *J* = 9.1 Hz, H5'), 7.31 (d, 1H, *J* = 8.8 Hz, H8); ^{13}C NMR ($CDCl_3$): δ = 159.5 (C2), 156.6 (C6'), 153.9 (C3'), 153.3 (C8a), 142.7 (C4), 136.2 (C7), 131.7 (C5), 129.3 (C4'), 128.2 (C5'), 122.8 (C3), 120.7 (C4a), 118.5 (C8), 117.9 (C6); HRMS (ESI): *m/z* $[M+H]^+$ calcd for $C_{13}H_7BrClN_2O_2$, 336.9373; found 336.9379.

Anal. Calcld for $C_{13}H_6BrClN_2O_2$: C, 46.26; H, 1.79; N, 8.30. Found: C, 46.35; H, 1.85; N, 8.25.

*4.2.3. 7-bromo-3-(6-chloropyridazin-3-yl)coumarin (**17c**).*

Brown solid; yield 54%; R_f = 0.5 (50% EtOAc/hexane); m.p. = 213 - 214 °C; ^{1}H NMR ($CDCl_3$): δ = 8.96 (s, 1H, H4), 8.56 (d, 1H, *J* = 9.1 Hz, H4'), 7.62 – 7.54 (m, 3H, H5', H5, H8), 7.50 (dd, 1H, *J* = 8.3, 1.7 Hz, H6); ^{13}C NMR ($CDCl_3$): δ = 159.3 (C2), 156.5 (C6'), 154.5 (C8a), 154.0 (C3'), 143.3 (C4), 130.4 (C5), 129.2 (C4'), 128.8 (C6), 128.2 (C5'), 127.7 (C7), 121.8 (C3), 120.1 (C8), 118.1 (C4a); HRMS (ESI): *m/z* $[M+H]^+$ calcd for $C_{13}H_7BrClN_2O_2$, 336.9373; found 336.9367.

Anal. Calcld for $C_{13}H_6BrClN_2O_2$: C, 46.26; H, 1.79; N, 8.30. Found: C, 46.40; H, 1.65; N, 8.49.

*4.2.4. 8-bromo-3-(6-chloropyridazin-3-yl)coumarin (**17d**)*

Brown solid; yield 51%; R_f = 0.5 (50% EtOAc/hexane); m.p. = 247 - 248 °C; ^{1}H NMR ($CDCl_3$): δ = 8.97 (s, 1H, H4), 8.58 (d, 1H, *J* = 9.1 Hz, H4'), 7.86 (dd, 1H, *J* = 7.9, 1.2 Hz, H7), 7.66 (dd, 1H, *J* = 7.9, 1.2 Hz, H5), 7.62 (d, 1H, *J* = 9.1 Hz, H5'), 7.26 (t, 1H, *J* = 7.9 Hz, H6); ^{13}C NMR ($CDCl_3$): δ = 159.1 (C2), 156.6 (C6'), 153.8 (C3'), 151.2 (C8a), 143.7 (C4), 136.8 (C7), 129.3 (C4'), 128.8 (C5), 128.2 (C5'), 125.9 (C6), 122.4 (C3), 120.4 (C4a), 110.3 (C8); HRMS (ESI): *m/z* $[M+H]^+$ calcd for $C_{13}H_7BrClN_2O_2$, 336.9374; found 336.9380.

Anal. Calcld for $C_{13}H_6BrClN_2O_2$: C, 46.26; H, 1.79; N, 8.30. Found: C, 46.45; H, 1.60; N, 8.42.

*4.2.5. 6-chloro-3-(6-chloropyridazin-3-yl)coumarin (**17e**).*

Brown solid; yield 56%; R_f = 0.6 (50% EtOAc/hexane); m.p. = 235 - 236 °C; ^{1}H NMR ($CDCl_3$): δ = 8.92 (s, 1H, H4), 8.56 (d, 1H, *J* = 9.1 Hz, H4'), 7.68 (d, 1H, *J* = 2.4 Hz, H5), 7.61 (d, 1H, *J* = 9.1 Hz, H5'), 7.58 (dd, 1H, *J* = 8.8, 2.8 Hz, H7), 7.37 (d, 1H, *J* = 8.8 Hz, H8); ^{13}C NMR ($CDCl_3$): δ = 159.5 (C2), 156.6 (C6'), 153.9 (C3'), 152.9 (C8a), 142.8 (C4), 133.4 (C7), 130.6 (C6), 129.3 (C4'), 128.6 (C5), 128.2 (C5'), 122.8 (C3),

120.2 (C4a), 118.2 (C8); HRMS (ESI): *m/z* $[M+H]^+$ calcd for $C_{13}H_7Cl_2N_2O_2$, 292.9879; found 292.9878.

Anal. Calcld for $C_{13}H_6Cl_2N_2O_2$: C, 53.27; H, 2.06; N, 9.56. Found: C, 53.40; H, 2.25; N, 9.42.

*4.2.5. 8-chloro-3-(6-chloropyridazin-3-yl)coumarin (**17f**).*

Brown solid; yield 64%; R_f = 0.6 (50% EtOAc/hexane); m.p. = 272 - 273 ºC; ^{1}H NMR ($CDCl_3$): δ = 9.00 (s, 1H, H4), 8.59 (d, 1H, *J* = 9.1 Hz, H4'), 7.70 (dd, 1H, *J* = 7.9, 1.4 Hz, H7), 7.66 - 7.57 (m, 2H, H5', H5), 7.32 (t, 1H, *J* = 7.9 Hz, H6); ^{13}C NMR ($CDCl_3$): δ = 159.0 (C2), 156.6 (C6'), 153.9 (C3'), 147.5 (C8a), 143.7 (C4), 133.6 (C7), 129.3 (C4'), 128.2, 128.0, 125.4 (C6), 122.4 (C3), 121.7 (C8), 120.4 (C4a); HRMS (ESI): *m/z* $[M+H]^+$ calcd for $C_{13}H_7Cl_2N_2O_2$, 292.9879; found 292.9887.

Anal. Calcld for $C_{13}H_6Cl_2N_2O_2$: C, 53.27; H, 2.06; N, 9.56. Found: C, 53.35; H, 1.90; N, 9.38.

*4.3. General methodology to synthesize the 3-(6-bromopyridazin-3-yl)coumarins (**18a-f**).*

An excess of $POBr_3$ (2.80 mmol) was added to a solution of the corresponding 3-(6-oxo-1,6-dihydropyridazin-3-yl)coumarin **21** (0.08 mmol) in toluene (4 mL). The reaction mixture was stirred under reflux for 8 h. The solvent was removed, H_2O (5 mL) was added, the precipitated formed was filtered and dried to provide the titled compound.

*4.3.1. 3-(6-bromopyridazin-3-yl)coumarin (**18a**).*

Brown solid; yield 48%; R_f = 0.5 (50% EtOAc/hexane); m.p. = 197 - 198 ºC; ^{1}H NMR ($CDCl_3$): δ = 9.00 (s, 1H, H4), 8.48 (d, 1H, *J* = 9.1 Hz, H4'), 7.76 - 7.67 (m, 2H, H5, H5'), 7.68 - 7.59 (m, 1H, H7), 7.44 - 7.32 (m, 2H, H6, H8); ^{13}C NMR ($CDCl_3$): δ = 159.9 (C2), 154.6, 154.5, 147.7 (C6'), 144.2 (C4), 133.5 (C7) 131.4 (C5'), 129.7 (C5), 129.0 (C4'), 125.3 (C6), 121.7 (C3), 119.2 (C4a), 116.8 (C8); HRMS (ESI): *m/z* $[M+H]^+$ calcd for $C_{13}H_8BrN_2O_2$, 302.9764; found 302.9768.

Anal. Calcld for $C_{13}H_7BrN_2O_2$: C, 51.51; H, 2.33; N, 9.24. Found: C, 51.65; H, 2.20; N, 9.39.

*4.3.2. 6-bromo-3-(6-bromopyridazin-3-yl) coumarin (**18b**).*

Brown solid; yield 60%; R_f = 0.6 (50% EtOAc/hexane); m.p. = 234 - 235 °C; ^{1}H NMR ($CDCl_3$): δ = 8.92 (s, 1H, H4), 8.46 (d, 1H, *J* = 9.1 Hz, H4'), 7.84 (d, 1H, *J* = 2.3 Hz, H5), 7.75 (d, 1H, *J* = 9.1 Hz, H5'), 7.72 (dd, 1H, *J* = 8.8, 2.2 Hz, H7), 7.31 (d, 1H, *J* = 8.8 Hz, H8); ^{13}C NMR ($CDCl_3$): δ = 159.4 (C2), 154.1 (C3'), 153.3 (C8a), 148.1 (C6'), 142.6 (C4), 136.2 (C7), 131.7, 131.5, 129.0 (C4'), 122.9 (C3), 120.7 (C4a), 118.5 (C8), 117.9 (C6); HRMS (ESI): *m/z* $[M+H]^+$ calcd for $C_{13}H_7Br_2N_2O_2$, 380.8869; found 380.8876.

Anal. Calcld for $C_{13}H_6Br_2N_2O_2$: C, 40.87; H, 1.58; N, 7.33. Found: C, 41.02; H, 1.39; N, 7.47.

*4.3.3. 7-bromo-3-(6-bromopyridazin-3-yl)coumarin (**18c**).*

Brown solid; yield 53%; R_f = 0.6 (50% EtOAc/hexane); m.p. = 182 - 183 °C; ^{1}H NMR ($CDCl_3$): δ = 8.97 (s, 1H, H4), 8.46 (d, 1H, *J* = 9.1 Hz, H4'), 7.74 (d, 1H, *J* = 9.1 Hz, H5'), 7.63 - 7.54 (m, 2H, H5, H8), 7.51 (dd, 1H, *J* = 8.3, 1.4 Hz, H6); ^{13}C NMR ($CDCl_3$): δ = 159.3 (C2), 154.5, 154.2, 147.9 (C6'), 143.3 (C4), 131.5 (C5'), 130.4 (C5), 128.9, 128.8, 127.8 (C7), 121.9 (C3), 120.1 (C8), 118.1 (C4a); HRMS (ESI): *m/z* $[M+H]^+$ calcd for $C_{13}H_7Br_2N_2O_2$, 380.8869; found 380.8861.

Anal. Calcld for $C_{13}H_6Br_2N_2O_2$: C, 40.87; H, 1.58; N, 7.33. Found: C, 40.69; H, 1.35; N, 7.19.

*4.3.4. 8-bromo-3-(6-bromopyridazin-3-yl)coumarin (**18d**).*

Brown solid; yield 72%; R_f = 0.4 (50% EtOAc/hexane); m.p. = 214 - 215 °C; ^{1}H NMR ($CDCl_3$): δ = 8.98 (s, 1H, H4), 8.48 (d, 1H, *J* = 9.1 Hz, H4'), 7.86 (dd, *J* = 7.9, 1.4 Hz, H7), 7.76 (d, 1H, *J* = 9.1 Hz, H5'), 7.66 (dd, 1H, *J* = 7.9, 1.4 Hz, H5), 7.26 (t, 1H, *J* = 7.9 Hz, H6); ^{13}C NMR ($CDCl_3$): δ = 159.1 (C2), 154.0 (C3'), 151.2 (C8a), 148.0 (C6'), 143.6 (C4), 136.8 (C7), 131.6 (C5'), 129.0, 128.8, 125.9 (C6), 122.5 (C3), 120.4 (C4a),

110.3 (C8); HRMS (ESI): *m/z* $[M+H]^+$ calcd for $C_{13}H_7Br_2N_2O_2$, 380.8869; found 380.8870.

Anal. Calcld for $C_{13}H_6Br_2N_2O_2$: C, 40.87; H, 1.58; N, 7.33. Found: C, 41.15; H, 1.42; N, 7.45.

*4.3.5. 3-(6-bromopyridazin-3-yl)-6-chlorocoumarin (**18e**).*

Brown solid; yield 82%; R_f = 0.6 (50% EtOAc/hexane); m.p. = 302 - 303 ºC; ^{1}H NMR ($CDCl_3$): δ = 8.93 (s, 1H, H4), 8.46 (d, 1H, *J* = 9.1 Hz, H4'), 7.75 (d, 1H, *J* = 9.1 Hz, H5'), 7.69 (d, 1H, *J* = 2.4 Hz, H5), 7.59 (dd, 1H, *J* = 8.8, 2.4 Hz, H7), 7.37 (d, 1H, *J* = 8.8 Hz, H8); ^{13}C NMR ($CDCl_3$): δ = 159.5 (C2), 154.1 (C3'), 152.8 (C8a), 148.1 (C6'), 142.8 (C4), 133.4 (C7), 131.5 (C5'), 130.7 (C6), 129.0 (C4'), 128.6 (C5), 122.9 (C3), 120.1 (C4a), 118.3 (C8); HRMS (ESI): *m/z* $[M+H]^+$ calcd for $C_{13}H_7BrClN_2O_2$, 336.9374; found 336.9387.

Anal. Calcld for $C_{13}H_6BrClN_2O_2$: C, 46.26; H, 1.79; N, 10.50. Found: C, 46.39; H, 1.56; N, 10.35.

*4.3.6. 3-(6-bromopyridazin-3-yl)-8-chlorocoumarin (**18f**).*

Brown solid; yield 95%; R_f = 0.5 (50% EtOAc/hexane); m.p. = 243 - 244 ºC; ^{1}H NMR ($CDCl_3$): δ = 8.99 (s, 1H, H4), 8.48 (d, 1H, *J* = 9.1 Hz, H4'), 7.76 (d, 1H, *J* = 9.1 Hz, H5'), 7.69 (dd, 1H, *J* = 7.9, 1.4 Hz, H7), 7.62 (dd, 1H, *J* = 7.9, 1.4 Hz, H5), 7.32 (t, 1H, *J* = 7.9 Hz, H6); ^{13}C NMR ($CDCl_3$): δ = 159.0 (C2), 154.0 (C3'), 150.1 (C8a), 148.0 (C6'), 143.6 (C4), 133.7 (C7), 131.5 (C5'), 129.0 (C4'), 128.1 (C5), 125.4 (C6), 122.5 (C3), 121.7 (C8), 120.4 (C4a); HRMS (ESI): *m/z* $[M+H]^+$ calcd for $C_{13}H_7BrClN_2O_2$, 336.9374; found 336.9375.

Anal. Calcld for $C_{13}H_6BrClN_2O_2$: C, 46.26; H, 1.79; N, 10.50. Found: C, 46.45; H, 1.96; N, 10.39.

4.4. In vitro assays

4.4.1. hMAO activity assays

The hMAO isoforms (Sigma-Aldrich SA) catalyze the oxidation of *p*-tyramine to cause the corresponding 4-hydroxyphenylacetaldehyde, ammonia and H_2O_2. The H_2O_2

produced can be detected by reaction with the Amplex® Red reagent (10-acetyl-3,7-dihydroxyphenoxazine) in the presence of horseradish peroxidase to produce a fluorescent substance, resorufin.

In order to determine the activity of compounds **17a-f** and **18a-f**, 0.1 mL of sodium phosphate buffer (50 mM, pH 7.4) containing different concentrations of the new compounds or reference inhibitors solved in DMSO (final concentration ≤ 1% DMSO), and hMAO-A or hMAO-B were incubated. The amount of hMAO-A or hMAO-B used was adjusted to obtain, in our experimental conditions, the same reaction rate: to oxidize (in the absence of the compounds: control group) the same substrate concentration: 165 pmoles of *p*-tyramine per minute (MAO-A; 1.1 µg; specific activity: 150 nmoles of oxidized *p*-tyramine to *p*-hydroxyphenylacetaldehyde/minute/mg protein; MAO-B: 7.5 µg; specific activity: 22 nmoles of *p*-tyramine transformed/minute/mg of protein). The incubation was performed for 10 minutes at 37 °C in black and flat bottom 96 well plates (MicrotestTM 96 well assay plate, BD Biosciences) placed in the dark chamber of the fluorescence reader. After the incubation period, the reaction was started by adding (final concentrations) 200 µM of Amplex® Red reagent, 1 unit (U)/mL of horseradish peroxidase and 1 mM of *p*-tyramine as a substrate.

The production of H_2O_2 and, consequently, of resorufin was quantified at 37 °C in a plate fluorescence reader (Fluo-star OptimaTM, BMG LABTECH) determining the fluorescence generated (excitation 545 nm, emission 590 nm) for 10 minutes, a period in which the increase in fluorescence was linear from the beginning. Simultaneously control experiments were carried out replacing our compounds or the reference inhibitors with the appropriate solutions of the vehicles. In addition, the possible ability of the new compounds to modify the fluorescence generated in the reaction mixture by a non-enzymatic inhibition (for example, by direct reaction with the Amplex® Red reagent), was evaluated by adding these compounds to solutions containing only the Amplex® Red reagent in sodium phosphate buffer.

MAO activity of the test compounds and reference inhibitors is expressed as IC_{50}, i.e., the concentration of each drug required to reduce 50% the control value activity for MAO isoforms.

4.4.2. Cytotoxicity assays.

The SH-SY5Y cells grew in a culture medium containing Nutrient Mixture F-12 Ham (Ham's F12) and Minimum Essential Medium Eagle (EMEM) (mixture 1:1) and

supplemented with 15% Fetal Bovine Serum (FBS), 1% L-Glutamine, 1% non-essential aminoacids (all of them from Sigma-Aldrich S.A.) and 1% of penicillin G/streptomycin sulfate (Gibco, Invitrogen).

The cells grew in 75 cm^2 flask in an incubator, under conditions of saturated humidity with a partial pressure of 5% CO_2 in the air, at 37 ºC, until reaching the confluence, 90-95% of the flask surface.

To carry out the cytotoxicity assays, the cells were seeded in sterile 96-well plates, with a density of $2x10^5$ cells/mL and grown distributed in aliquots of 100 µL for 24 h under the conditions above described.

Subsequently, the cultures were treated with the compounds dissolved in DMSO, at 10 µM concentration (1% DMSO/100 µL well) and incubated for 24 h. After this time, cell viability was determined using MTT (5 mg/mL in Hank's). 10 µL of MTT solution were added to each well containing 100 µL of culture medium and the cells were incubated for 2 h as above described. Then, culture medium was removed, 100 µL DMSO/well was added to solve the formazan crystals formed by the viable cells and the absorbance (λ 540 nm) was quantified in a plate reader. The viability (percentage) was calculated as [Absorbance (treatment)/Absorbance (negative control)]100%.

4.5. In vivo assays

4.5.1. Animals

Swiss male mice with a weight of 25 ± 5 g were used. The minimum number of animals used in each experiment was 8 (n = 8).

The stabling, handling and the different experimental techniques were carried out in accordance with Directive 2010/63/EU of the European Parliament and of the Council of September 22, 2010, on the protection of animals used for scientific purposes, and Royal Decree 53/2013 of February 1, which establishes the basic rules applicable to the protection of animals used in experimentation and other scientific purposes, including teaching and the Guide for the care and use of animals Laboratory developed by AAALAC International (Association for Assessment and Accreditation of Laboratory Animal Care International, International Association for the Evaluation and Accreditation of Laboratory Animal Care).

The experiments were carried out following the procedure informed with Registration Code 15007AE/09/INV MED 02/NER02/JAFG4, authorized by the Consellería do Medio Rural - Autonomous Government of Galicia (Xunta de Galicia).

The mice were housed in standard Makrolon cages (215x465x145 mm^3) without any restriction on access to food and water, except during the realization of experiment.

Prior to conducting the experiments, the animals were acclimatized, for a minimum of 72 hours, to the environmental conditions in a silent, thermostatted chamber (22 ± 1 ºC), with a 12-hour light/dark cycle (08:00 h - 20:00 h) and with humidity controlled (45 - 65%).

The experiments were always carried out at the same time of the day in order to avoid possible modifications due to circadian cycles. The mice were used only once to avoid alterations in the response due to tolerance or learning phenomena.

4.5.2. Equipment

The evaluation of the motor activity in mice was performed using the Open Field Test (OFT).

For the experiment, the animals were placed in a black square box of size 1x1x0.30 m^3, subdivided into 4 independent arenas (0.50x0.50x0.30 m^3) where every mouse was placed independently.

The evaluation in the OFT was carried out from a room adjacent to the one conducting the experiment using a video registration system. The behavior of the animals was captured with an analog camcorder (Sony DXC-107A, Sony Corporation, Japan) suspended on the ceiling. The camera is connected to an adapter (Sony CMA D2) that sends the signal to a monitor (Sony PVM-14M2E) and to two digitizing cards:

i. An internal one located in a PCI slot of the computer (Picolo frame graber, Euresys, Liege, Belgium).

ii. Another external with USB connection (DVC-USB, Dazzle, USA).

The direct signal of the Picolo card is used by the videocomputerized animal observation system (EthoVision V. 3.1.16, Noldus Information Technology, Wageningen, The Netherlands). The EthoVision software locates the center of the animal, stores the data and allows further analysis.

4.5.3. Protocol

Animal models used were unpretreated mice and reserpinized mice, last were used as a model of PD.

A suspension of 1% carboxymethylcellulose sodium (CMCNa) was used as control while selegiline was used as MAO-B drug baseline. Compound **18c** was tested at doses of 10 and 100 mg/kg, in a suspension of 1% CMCNa.

Four independent groups ($n \geq 8$) of unpretreated mice were administered the vehicle (1% CMCNa i.p.), the reference drug (selegiline, 10 mg/kg, i.p.) or compound **18c** (100 or 10 mg/kg, i.p.) in a volume/animal weight ratio of 10 mL/kg.

The pharmacological model of PD consisted on the administration of reserpine (1.25 mg/kg, i.p.) to the animals 22 hours before the experiment. After that time, six independent groups were established. Two of them were treated with the vehicle (1% CMCNa ip), other two received selegiline (10 mg/kg) and the last two were treated with **18c** (100 mg/kg or 10 mg/kg i.p). After 30 min, L-dopa/benserazide (100:25 mg/kg, i.p.) were injected to the four groups of mice pretreated with selegiline or compound **18c**. The other two groups were again injected with the vehicle.

Half an hour after the last administration, the evaluation of the motor activity started for a period of one hour. The parameters evaluated were: locomotor activity (cm/h), velocity (cm/s), percentage of time in movement (%).

The graphical representation and statistical analysis were performed using GraphPad Prism (V 6.0) (San Diego, USA). Statistically significant differences were determined by one-way ANOVA followed by the Dunnett test.

4.6. Molecular modeling

All the synthesized compounds were built and their partial charges calculated after semi-empirical (PM6) energy minimization using MOE2018.01 [24]. The co-crystallized hMAO-B structure (PDB code: 2V60) bound to the coumarin 7-(3-chlorobenzyloxy)-4-carboxaldehydecoumarin (c17) was identified for the docking simulations [22]. The hMAO-B structure was prepared with the Protein Preparation Tool available in the MOE suite. Briefly, the protein preparation procedure included the addition and optimization of hydrogens, chain termini capping, optimization of protonation state by protonate-3D tool, modeling the missing atoms (i.e. Ile501.A), partial charges calculations. The most suitable docking protocol was identified using a benchmark over 17 protein/scoring protocol using DockBench 1.06 [25], a tool that

compares the performance of different posing/scoring protocols on two hMAO-B complexes containing two coumarin scaffold ligands (PDB code: 2v60, 2v61). The benchmark suggested GOLD [26] as docking engine coupled to Chemscore as a scoring function; each ligand was docked 20 times and finally rescored by MOE by London dG [24]. To facilitate the visualization and analysis of data obtained from the docking simulations, we produced a video that shows the most relevant docking data, such as docking poses, per residue IEhyd and IEele data, experimental binding data and scoring values. ADME descriptors were predicted by the Stardrop software package [27].

Acknowledgments

Financial support from Universidade de Vigo, the Consellería de Cultura, Educación e Ordenación Universitaria (CN2012/184, and EM2014/016 and Centro singular de investigación de Galicia acreditación 2016-2019, ED431G/05) and the European Regional Development Fund (ERDF), is gratefully acknowledged. M.C.C.-L. thanks the Xunta de Galicia for her PhD fellowship.

Supplementary Information

References

[1] R. Scatena, G. E. Martorana, P. Bottoni, G. Botta, P. Pastore, B. Giardina, An update on pharmacological approaches to neurodegenerative diseases, Expert Opin. Investig. Drugs 16 (2007) 59-72, https://doi.org/10.1517/13543784.16.1.59.

[2] C. Soto, Unfolding the role of protein misfolding in neurodegenerative diseases, Nat. Rev. Neurosci. 4 (2003) 49-60, https://doi.org/10.1038/nrn1007.

[3] S. Ma, I. Y. Attarwala, X. Q. Xie, SQSTM1/p62: a potential target for neurodegenerative disease**,** ACS Chem. Neurosci. 10 (2019) 2094-2114, https://doi.org/10.1021/acschemneuro.8b00516.

[4] L. V. Kalia, A. E. Lang, Parkinson's disease, Lancet 386 (2015) 896-912, https://doi.org/10.1016/S0140-6736(14)61393-3.

[5] a) M. Rosini, E. Simoni, A. Milelli, A. Minarini, C. Melchiorre, Oxidative stress in Alzheimer's disease: are we connecting the dots?, J. Med. Chem. 57 (2014) 2821-2831, https://doi.org/10.1021/jm400970m; b) F. T. Zindo, S. F. Malan, S. I. Omorugy, A. B. Enogieru, Design, synthesis and evaluation of pentacycloundecane and

hexacycloundecane propargylamine derivatives as multifunctional neuroprotective agents, Eur. J. Med. Chem. 163 (2019) 83-94, https://doi.org/10.1016/j.ejmech.2018.11.051; c) P. Jenner, Istradefylline, a novel adenosine A_{2A} receptor antagonist, for the treatment of Parkinson's disease, Expert Opin. Investig. Drugs 14 (2005) 729-738, https://doi.org/10.1517/13543784.14.6.729; d) A. Affini, S. Hagenow, A. Zivkovic, J. Marco-Contelles, H. Stark, Novel indanone derivatives as MAO B/H_3R dual-targeting ligands for treatment of Parkinson's disease, Eur. J. Med. Chem. 148 (2018) 487-497, https://doi.org/10.1016/j.ejmech.2018.02.015.

[6] a) L. M. Ellis, M. J. Fell, Current approaches to the treatment of Parkinson's disease, Bioorg. Med. Chem. Lett. 27 (2017) 4247-4255, https://doi.org/10.1016/j.bmcl.2017.07.075; b) A. Salamon, D. Zádori, L. Szpishak, P. Klibenyi, L. Vecsei, Opicapone for the treatment of Parkinson's disease: an update, Expert Opin. Pharmacother. 20 (2019) 2201-2207, https://doi.org/10.1080/14656566.2019.1681971.

[7] L. Dézsi, L. Vécsei, Monoamine oxidase B inhibitors in Parkinson's disease, CNS Neurol. Disord. Drug Targets 16 (2017) 425-439 https://doi.org/10.2174/1871527316666170124165222.

[8] D. E. Edmonson, C. Binda, Monoamine Oxidases, In: Harris J., Boekema E. (eds) Membrane Protein Complexes: Structure and Function, Subcell. Biochem. vol 87, vol 87. Springer, Singapore 2018, pp. 117-139.

[9] a) A. Marzo, L. Dal Bo, N. C. Monti, F. Crivelli, S. Ismaili, C. Caccia, C. Cattaneo, R. G. Fariello, Pharmacokinetics and pharmacodynamics of safinamide, a neuroprotectant with antiparkinsonian and anticonvulsant activity, Pharmacol. Res. 50 (2004) 77-85, https://doi.org/10.1016/j.phrs.2003.12.004; b) A. Kupsch, J. Sautter, M. E. Götz, W. Breithaupt, J. Schwarz, M. B. Youdim, P. Riederer, M. Gerlach, W. H. Oertel, Monoamine oxidase-inhibition and MPTP-induced neurotoxicity in the non-human primate: comparison of rasagiline (TVP 1012) with selegiline, J. Neural. Transm. (Vienna). 108 (2001) 985-1009, https://doi.org/10.1007/s007020170018.

[10] T. Müller, Safinamide for symptoms of Parkinson's disease, Drugs Today 51 (2015) 653-659, https://doi.org/10.1358/dot.2015.51.11.2414529.

[11] a) S. Sturm, A. Forsberg, S. Nave, P. Stenkrona, N. Seneca, A. Varrone, R. A. Comley, P. Fazio, C. Jamois, R. Nakao, Z. Ejduk, N. Al-Tawil, U. Akenine, C. Halldin, N. Andreasen, B. Ricci, Positron emission tomography measurement of brain MAO-B inhibition in patients with Alzheimer's disease and elderly controls after oral

administration of sembragiline, Eur. J. Nucl. Med. Mol. Imaging 44 (2017) 382-391, https://doi.org/10.1007/s00259-016-3510-6; b) S. Nave, R. S. Doody, M. Boada, T. Grimmer, J. M. Savola, P. Delmar, M. Pauly-Evers, T. Nikolcheva, C. Czech, E. Borroni, B. Ricci, J. Dukart, M. Mannino, T. Carey, E. Moran, I. Gilaberte, N. Milani-Muelhardt, I. Gerlach, L. Santarelli, S. Ostrowitzki, P. Fontoura, Sembragiline in moderate Alzheimer's disease: results of a randomized, double-blind, placebo-controlled phase II trial (MAyflOwer RoAD), J. Alzheimer's Dis. 58 (2017) 1217-1228, http://dx.doi.org/10.3233/JAD-161309.

[12] a) F. Borges, F. Roleira, N. Milhazes, L. Santana, E. Uriarte, Simple coumarins: privileged scaffolds in medicinal chemistry, Front. Med. Chem. 4 (2009) 23-85, doi: 10.2174/978160805207310904010023; b) I. Erdogan Orhan, H. Ozan Gulcan, Coumarins: auspicious cholinesterase and monoamine oxidase inhibitors, Curr. Top. Med. Chem. 15(2015) 1673-1682, doi: 10.2174/1568026615666150427113103; c) S. Emami, S. Dadashpour, Current developments of coumarin-based anti-cancer agents in medicinal chemistry, Eur. J. Med. Chem. 102 (2015) 611-630, https://doi.org/10.1016/j.ejmech.2015.08.033; d) M. Kumar Gupta, S. Kumar, S. Chaudhary, Coumarins: a unique scaffold with versatile biological behavior, Asian J. Pharm. Clin. Res. 12 (2019) 27-38, https://doi.org/10.22159/ajpcr.2019.v12i3.30635.

[13] a) S. Carradori, R. Silvestri, New frontiers in selective human MAO-B inhibitors, J. Med. Chem. 58 (2015) 6717-6732, https://doi.org/10.1021/jm501690r; b) A. Stefanachi, F. Leoneti, L. Pisani, M. Catto, A. Carotti, Coumarin: a natural, privileged and versatile scaffold for bioactive compounds**,** Molecules 23 (2018) 250, https://doi.org/10.3390/molecules23020250.

[14] a) M. J. Matos, C. Terán, Y. Pérez-Castillo, E. Uriarte, L. Santana, D. Viña, Synthesis and study of a series of 3-arylcoumarins as potent and selective monoamine oxidase B inhibitors, J. Med. Chem. 54 (2011) 7127-7137, https://doi.org/10.1021/jm200716y; b) M. J. Matos, S. Vilar, V. García-Morales, N. P. Tatonetti, E. Uriarte, L. Santana, D. Viña, Insight into the functional and structural properties of 3-arylcoumarin as an interesting scaffold in monoamine oxidase B inhibition**,** ChemMedChem 9 (2014) 1488-1500, https://doi.org/10.1002/cmdc.201300533.

[15] a) G. Delogu, C. Picciau, G. Ferino, E. Quezada, G. Podda, E. Uriarte, D. Viña, Synthesis, human monoamine oxidase inhibitory activity and molecular docking studies of 3-heteroarylcoumarin derivatives, Eur. J. Med. Chem. 46 (2011) 1147-1152,

https://doi.org/10.1016/j.ejmech.2011.01.033; b) M. C. Costas-Lago, P. Besada, F. Rodríguez-Enríquez, D. Viña, S. Vilar, E. Uriarte, F. Borges, C. Terán, Synthesis and structure-activity relationship study of novel 3-heteroarylcoumarins based on pyridazine scaffold as selective MAO-B inhibitors, Eur. J. Med. Chem. 139 (2017) 1-11, https://doi.org/10.1016/j.ejmech.2017.07.045.

[16] M. C. Costas-Lago, P. Besada, E. Cano, C. Terán, Novel compounds of hybrid structure pyridazinone-coumarin as potent inhibitors of platelet aggregation, Future Med. Chem. 11 (2019) 2051-2062, https://doi.org/10.4155/fmc-2018-0373.

[17] R. A. Copeland, Evaluation of Enzyme Inhibitors in Drug Discovery: A Guide for Medicinal Chemists and Pharmacologists, 2nd Edition, Wiley-Interscience, Hoboken, 2013.

[18] Y. Liu, D. A. Peterson, H. Kimura, D. Schubert, Mechanism of cellular 3-(4,5-dimethylthiazol-2-yl)-2,5-diphenyltetrazolium bromide (MTT) reduction**,** J. Neurochem. 69 (1997) 581-593, https://doi.org/10.1046/j.1471-4159.1997.69020581.x.

[19] M. J. Matos, S. Vilar, R. M. González-Franco, E. Uriarte, L. Santana, C. Friedman, N. P. Tatonetti, D. Viña, J. A. Fontenla, Novel (coumarin-3-yl)carbamates as selective MAO-B inhibitors: synthesis, in vitro and in vivo assays, theoretical evaluation of ADME properties and docking study, Eur. J. Med. Chem. 63 (2013) 151-161, https://doi.org/10.1016/j.ejmech.2013.02.009.

[20] G. Engberg, T. Elebring, H. Nissbrandt, Deprenyl (selegiline), a selective MAO-B inhibitor with active metabolites; effects on locomotor activity, dopaminergic neurotransmission and firing rate of nigral dopamine neurons**,** J. Pharmacol. Exp. Ther. 259 (1991) 841-847.

[21] G. Englund, P. Lundquist, C. Skogastierna, J. Johansson, J. Hoogstraate, L. Afzelius, T. B. Andersson, D. Projean, Cytochrome P450 inhibitory properties of common efflux transporter inhibitors**,** drug metab. dispos. 42 (2014) 441–447, https://doi.org/10.1124/dmd.113.054932.

[22] C. Binda, J. Wang, L. Pisani, C. Caccia, A. Carotti, P. Salvati, D. E. Edmondson, A. Mattevi, Structures of human monoamine oxidase B complexes with selective noncovalent inhibitors: safinamide and coumarin analogs, J. Med. Chem. 50 (2007) 5848-5852, https://doi.org/10.1021/jm070677y.

[23] B. Mathew, S. Carradori, P. Guglielmi, M.S. Uddin MS, H. Kim, New Aspects of monoamine oxidase B inhibitors: the key role of halogens to open the golden door, Curr. Med. Chem. (2020) 27: 1. https://doi.org/10.2174/0929867327666200121165931.

[24] Chemical Computing Group (CCG) Inc., Molecular Operating Environment (MOE), (2018). http://www.chemcomp.com.

[25] A. Cuzzolin, M. Sturlese, I. Malvacio, A. Ciancetta, S. Moro, DockBench: an integrated informatic platform bridging the gap between the robust validation of docking protocols and virtual screening simulations, Molecules 20 (2015) 9977–9993, https://doi.org/10.3390/molecules20069977.

[26] M. L. Verdonk, J. C. Cole, M. J. Hartshorn, C. W. Murray, R. D. Taylor, Improved protein-ligand docking using GOLD, Proteins 52 (2003) 609–623, https://doi.org/10.1002/prot.10465.

[27] StardropTM, version 6.4, (n.d.). http://www.optibrium.com/stardrop/stardrop-adme-qsar-models.php.

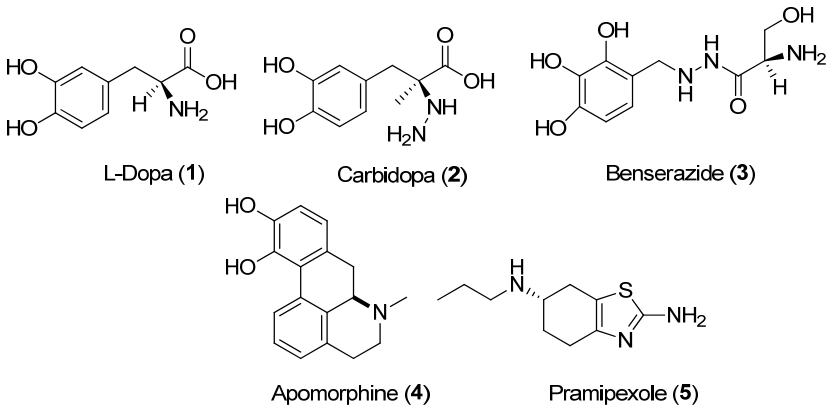

Figure 1. Dopamine precursor (compound **1**), peripheral decarboxylase inhibitors (compounds **2-3**) and dopamine agonists (compounds **4-5**) used in PD therapy

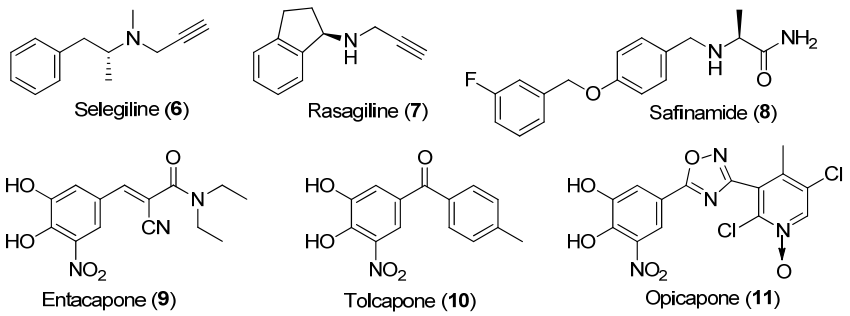

Figure 2. Selection of MAO-B (compounds **6-8**) and COMT inhibitors (compounds **9-11**) approved for PD therapy

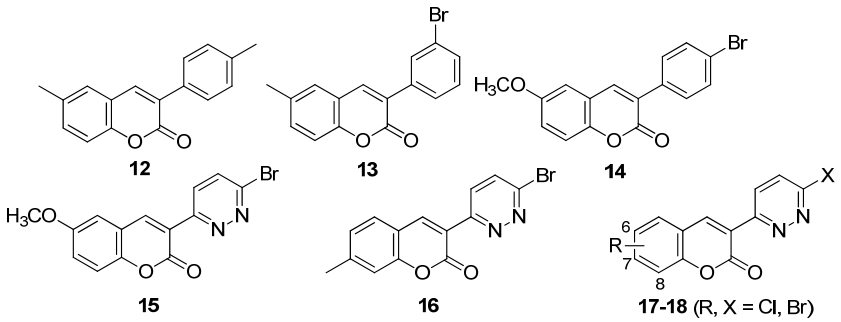

Figure 3. Structure of several 3-arylcoumarins (compounds **12**-**14**) and of some of their pyridazinyl analogues (compounds **15**-**16**) described as MAO-B inhibitors and general structure of the novel 3-pyridazinylcoumarins proposed (compounds **17**-**18**).

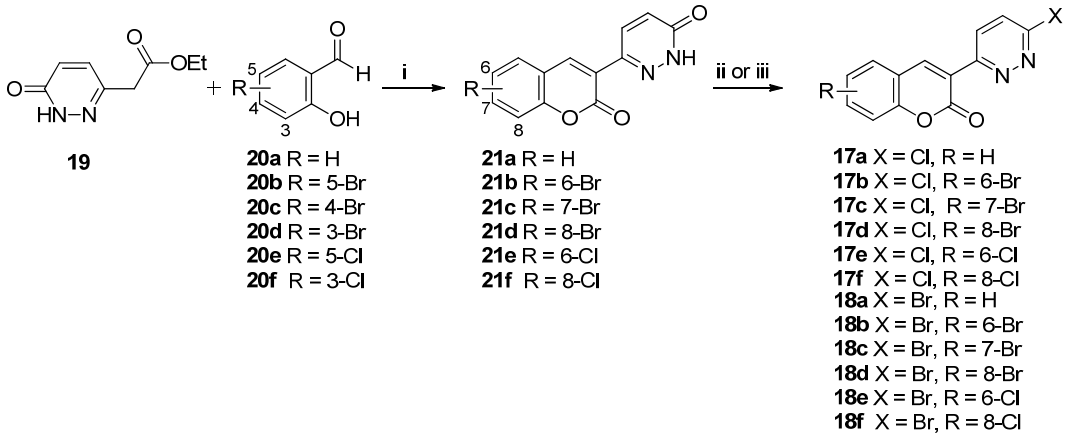

Scheme 1. Reagents and conditions: (i) piperidine, 2-propanol, reflux, 5 h, 86% (**21a**), 78% (**21b**), 83% (**21c**), 81% (**21d**), 73% (**21e**), 87% (**21f**); (ii) $POCl_3$, reflux, 14 h, 51% (**17a**), 61% (**17b**), 54% (**17c**), 51% (**17d**), 56% (**17e**), 64% (**17f**); (iii) $POBr_3$, toluene, reflux, 8 h, 48% (**18a**), 60% (**18b**), 53% (**18c**), 72% (**18d**), 82% (**18e**), 95% (**18f**).

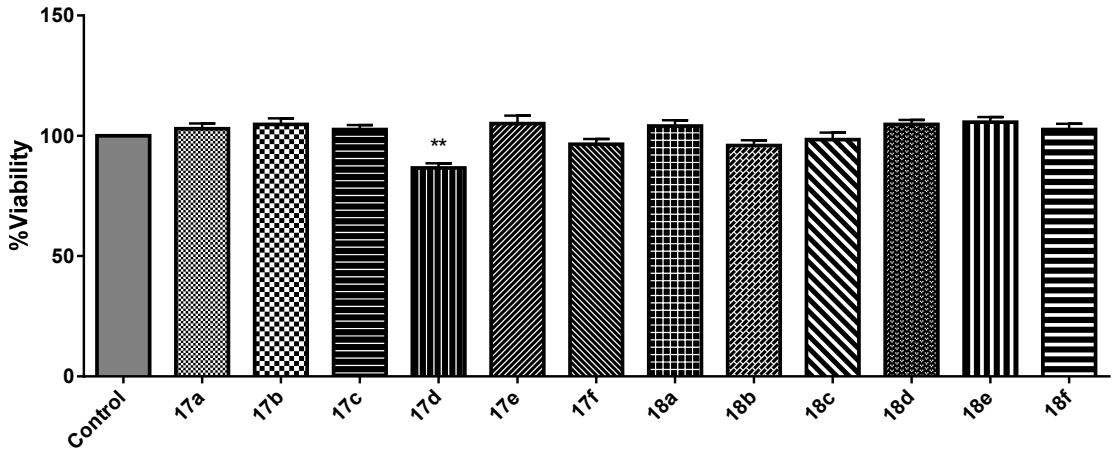

Figure 4. Cytotoxic activity of compounds **17a-f** and **18a-f** (10 µM) on SH-SY5Y cells after 24 h incubation. Results are expressed as mean ± s.e.m. from at least 5 different cultures. **P ≤ 0.05 versus the control group treated with vehicle (DMSO 1%). Comparisons were performed by one-way ANOVA followed by Dunnett's multiple comparisons test.

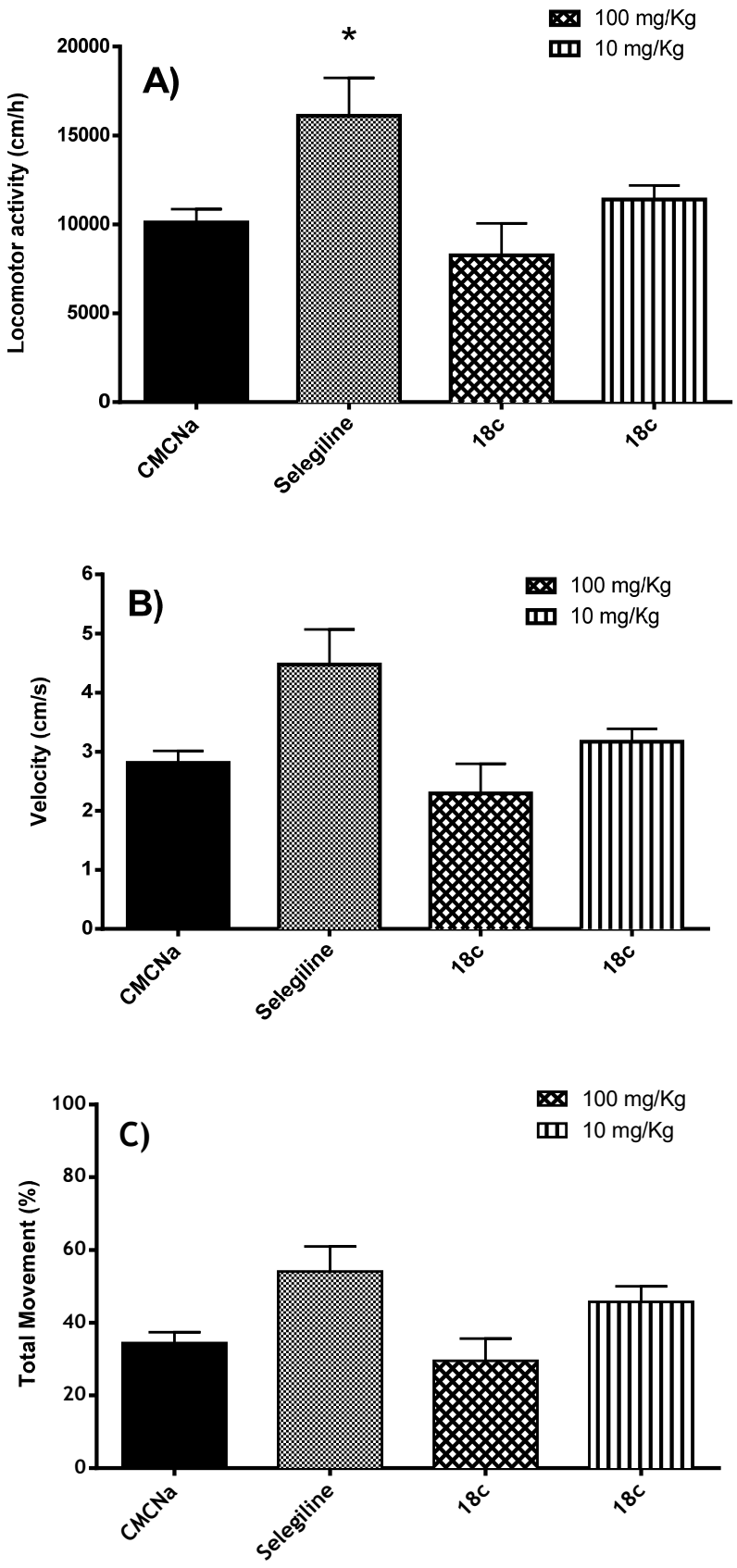

Figure 5. Results obtained in the Open Field Test (OFT) in unpretreated mice. Selegiline (10 mg/kg), compound **18c** (100 mg/kg and 10 mg/kg) (**A**) Locomotor activity (cm/h), (**B**) velocity (cm/s) and (**C**) total movement (%).*$P < 0.05$.

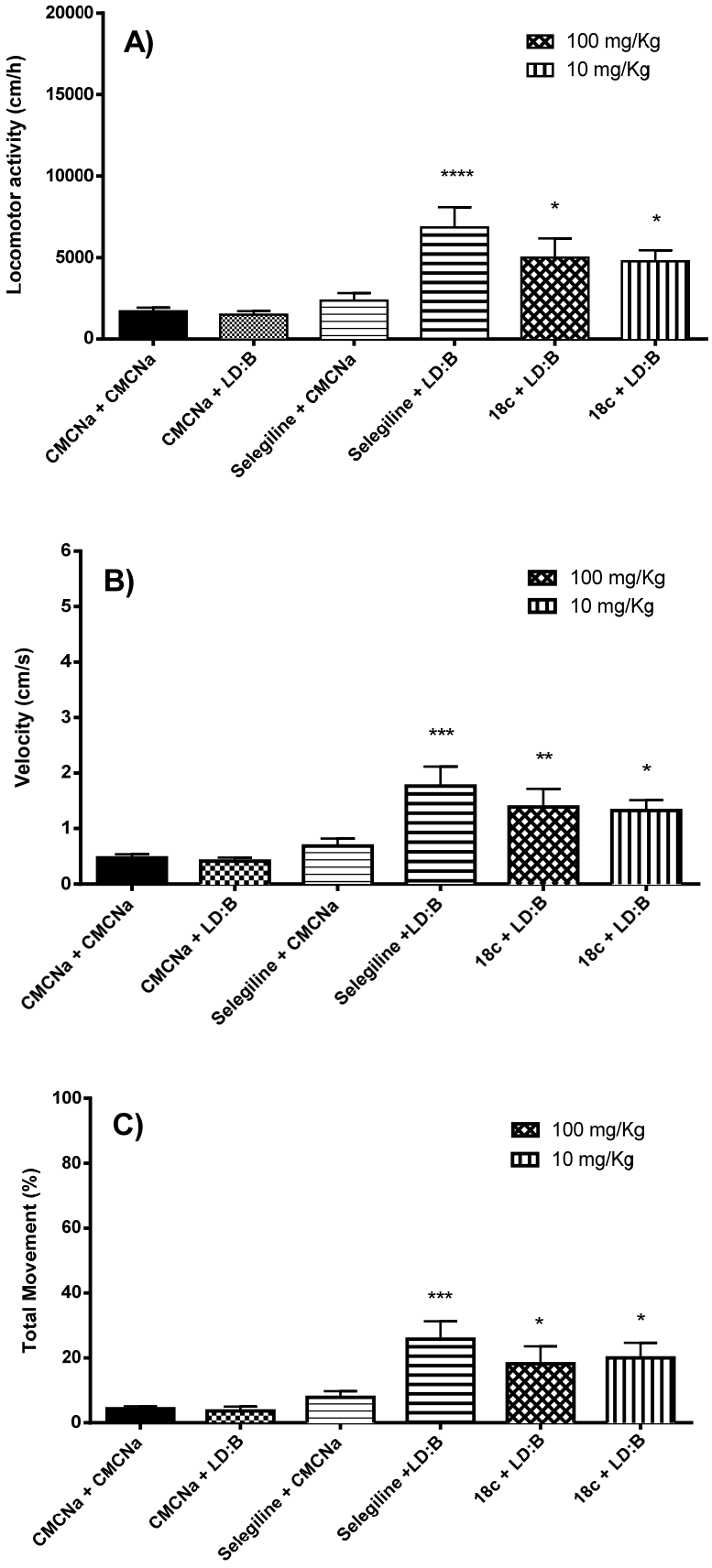

Figure 6. Results obtained in mice pretreated with reserpine, LD/B and selegiline (10 mg/kg), or compound **18c** (100 mg/kg and 10 mg/kg) (**A**) Locomotor activity (cm/h), (**B**) velocity (cm/s) and (**C**) total movement (%).*** P<0.001; *P<0.05.

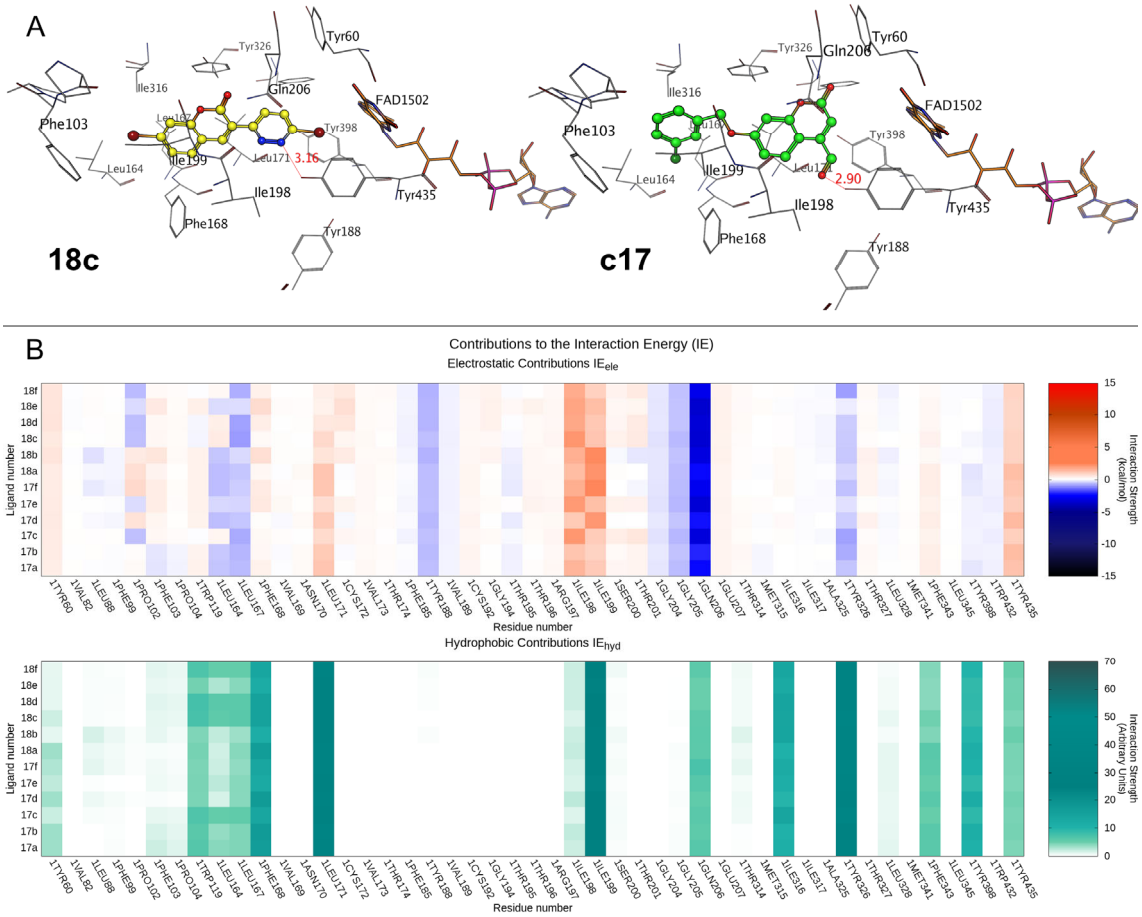

Figure 7. Panel A, the pose of **18c** (in yellow) is compared to the crystallographic conformation of c17 (PDB ID: 2v60, in green). In Panel B it is reported the contribution of each residue to the interaction energy focusing to the electrostatic and hydrophobic interactions. The strength of the IE_{ele} and IE_{hyd} contribution is color-coded according to their strength computed by MOE scoring function.